Neuroscience Letters 830 (2024) 137778

Contents lists available at ScienceDirect

Neuroscience Letters

journal homepage: www.elsevier.com/locate/neulet

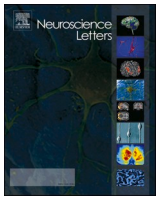

Research article

Unraveling the CLCC1 interactome: Impact of the Asp25Glu variant and its interaction with SigmaR1 at the Mitochondrial-Associated ER Membrane (MAM)

Ilaria D'Atri [a,b], Emily-Rose Martin [b], Liming Yang [b], Elizabeth Sears [b], Emma Baple [b], Andrew H. Crosby [b], John K. Chilton [d], Asami Oguro-Ando [b,c,*]

[a] School of Physiology, Pharmacology and Neuroscience, University of Bristol, BS8 1TD, United Kingdom
[b] University of Exeter Medical School, University of Exeter, Exeter, United Kingdom
[c] Laboratory of Pharmacology, Faculty of Pharmaceutical Science, Tokyo University of Science, Japan
[d] Peninsula Medical School, University of Plymouth, Plymouth, United Kingdom

ARTICLE INFO

Keywords:
CLCC1
Endoplasmic reticulum
SigmaR1
MAM
Retinitis pigmentosa

ABSTRACT

The endoplasmic reticulum (ER) plays an indispensable role in cellular processes, including maintenance of calcium homeostasis, and protein folding, synthesized and processing. Disruptions in these processes leading to ER stress and the accumulation of misfolded proteins can instigate the unfolded protein response (UPR), culminating in either restoration of balanced proteostasis or apoptosis. A key player in this intricate balance is CLCC1, an ER-resident chloride channel, whose essential role extends to retinal development, regulation of ER stress, and UPR. The importance of CLCC1 is further underscored by its interaction with proteins localized to mitochondria-associated endoplasmic reticulum membranes (MAMs), where it participates in UPR induction by MAM proteins.

In previous research, we identified a p.(Asp25Glu) pathogenic CLCC1 variant associated with retinitis pigmentosa (RP) (CLCC1 hg38 NC_000001.11; NM_001048210.3, c.75C > A; UniprotKB Q96S66). In attempt to decipher the impact of this variant function, we leveraged liquid chromatography-mass spectrometry (LC-MS) to identify likely CLCC1-interacting proteins. We discovered that the CLCC1 interactome is substantially composed of proteins that localize to ER compartments and that the Asp25Glu variant results in noticeable loss and gain of specific protein interactors. Intriguingly, the analysis suggests that the CLCC1Asp25Glu mutant protein exhibits a propensity for increased interactions with cytoplasmic proteins compared to its wild-type counterpart.

To corroborate our LC-MS data, we further scrutinized two novel CLCC1 interactors, Calnexin and SigmaR1, chaperone proteins that localize to the ER and MAMs. Through microscopy, we demonstrate that CLCC1 co-localizes with both proteins, thereby validating our initial findings. Moreover, our results reveal that CLCC1 co-localizes with SigmaR1 not merely at the ER, but also at MAMs. These findings reinforce the notion of CLCC1 interacting with MAM proteins at the ER-mitochondria interface, setting the stage for further exploration into how these interactions impact ER or mitochondria function and lead to retinal degenerative disease when impaired.

1. Background

In eukaryotes the endoplasmic reticulum (ER) is the organelle where calcium homeostasis is maintained, and lipids or proteins are produced, modified, exported, and degraded [1–3]. The folding of proteins is a necessary step for export or membrane insertion, and failure of this process leads to accumulation of misfolded proteins [3,4]. When the demand for the secretion of folded proteins and the accumulation of misfolded proteins occurs, the ER undergoes stress [4,5]. Pathways of stress signaling, collectively called the unfolded protein response (UPR), are activated to restore homeostasis and survival of the cell or induce apoptosis, leading to cell death [5,6].

Many proteins have been identified to be fundamental for retinal development and function (for example RHO, RP1, ATF6, CLCC1, etc.)

* Corresponding author at: University of Exeter Medical School, University of Exeter, Exeter, United Kingdom.
E-mail address: A.Oguro-Ando@exeter.ac.uk (A. Oguro-Ando).

https://doi.org/10.1016/j.neulet.2024.137778
Received 4 September 2023; Received in revised form 23 March 2024; Accepted 12 April 2024
Available online 15 April 2024

[7–10]. One of these, CLCC1, is an ER-resident chloride channel, and variants in it have been associated with neurodegeneration of the retina [11]. Although the variant (referred to as the Asp25Glu variant) results in pathological events, its expression is necessary for development [7]. We have previously shown that loss of function of CLCC1 during development in both mouse and zebrafish is lethal, while heterozygous knockout or knockdown negatively impact the development of the retina [7]. Specifically, cone and rod photoreceptors fail to develop, with fewer number of them being functional [7].

As mentioned above, CLCC1 localizes in the ER, and the loss of CLCC1 was linked with increase of UPR response and ER stress [7]. CLCC1 loss of function has also been reported to increase the levels of ER chaperone BiP (GRP78), consistent with the induction of ER stress [12]. Recently, Chu *et al.* [13] demonstrated that CLCC1 interacts with the microprotein PIGBOS at ER-mitochondria contact sites, where CLCC1 is necessary for PIGBOS to function as an UPR activator. In this work, we looked for binding partners of CLCC1 using mass spectrometry and validate novel CLCC1-interacting proteins by immunoprecipitation and microscopy. We observe that CLCC1 co-localizes and co-precipitates with Calnexin; as well as Sigma Non-Opioid Intracellular Receptor 1 (SigmaR1), an ER chaperone protein that localizes to mitochondria-associated endoplasmic reticulum membranes (MAMs). These results support the finding of CLCC1 interacting with MAM proteins at the interface between the ER and mitochondria.

2. Method details

2.1. Plasmid cloning

Flag-tagged CLCC1 and YFP-tagged CLCC1 plasmid were previously described in [7]. YFP-CLCC1 isoforms were cloned in pClink using the following primers.

Forward:
5′-ATATAAGCTTGGACTTTTTCATGATTTTGAAACATGGAAGTGGC-3′ (Isoform 2)
5′-ATATAAGCTTGGACTTCTAGCTTTTGCACAGCATCAGGCTGAAG-5′ (Isoform 3)
5′-ATATAAGCTTGGACTTGCACTTGCAGTTACATTCACCACATTGG-5′ (Isoform 4)

Reverse:
3′-ATTAGTCGACCTAGCAGGGGCTGCTGACCGG-5′

2.2. Cell culture and transfection

HEK293 and NIH/3T3 cells were cultivated in DMEM (#BE15-604D, *Lonza Bioscience*) supplemented with 10 U/mL of penicillin/streptomycin (#17–602, *Lonza Bioscience*) and 10 % fetal bovine serum (#16140071, *Gibco*™) in incubators at 37 °C with 5 % CO_2. Cells were maintained in 10-cm-diameter Petri dishes and passaged at 70–80 % confluency by trypsinization (#CC-5002, *Lonza Bioscience*) for 5 min at 37 °C before inactivation with an equal volume of culture media.

Cells were transfected with plasmid DNA encoding FLAG-tagged $CLCC1^{WT}$ protein (specifically, isoform 1) or the FLAG-tagged $CLCC1^{Asp25Glu}$ mutant using Lipofectamine™ LTX (#A12621, *Invitrogen*™) following manufacturer instructions. Following 24 h of FLAG fusion protein expression, cells were fixed with 4 % paraformaldehyde (PFA) (#158127, *Sigma Aldrich*®) for 15 min at room temperature for immunostaining or lysed for immunoprecipitation of CLCC1. Isoform 1 of CLCC1 was chosen as this is the only isoform that is affected by the Asp25Glu variant.

MitoTracker™ Red CMXRos (#M7512, *Invitrogen*™) was dissolved in DMSO and used at a final concentration of 150 nM. Cells were treated with MitoTracker™ for 15 min at 37 °C before fixation.

2.3. Immunoprecipitation, LC-MS and LC-MS data analysis

HEK293 cells were seeded and transfected at 60–70 % confluency in 10-cm-diameter Petri dishes 24 h prior to lysis. Immunoprecipitation of FLAG-tagged proteins was performed using Dynabeads™ Protein A (#10001D, *Invitrogen*™). 25 µL of Dynabead™ slurry was transferred to a clean microcentrifuge tube, and beads pelleted by centrifugation at 700×g for 1 min at 4 °C. The supernatant was removed and 200 µL of 1:1,000 diluted anti-FLAG antibody (#F1804, *Sigma Aldrich*®) in 1×PBS with 0.02 % Tween®-20 (#P1379, *Sigma Aldrich*®) (henceforth referred to as PBS-T) was added to the beads, and the antibody/Dynabead™ incubated at room temperature for 1 h, rotating end-over-end.

During bead-antibody complexing, transfected HEK293 cells were harvested by trypsinization and pelleted by centrifugation at 200×g for 5 min. The cell pellet was washed with ice-cold 1×PBS (#BE17-516F, *Lonza Bioscience)* prior to incubation with 400 µL of lysis buffer (20 mM Tris-HCl (#T1503, *Sigma Aldrich*®) pH = 8.0, 150 mM KCl (#P9541, *Sigma Aldrich*®), 0.1 % Triton™ X-100 (#T8787, *Sigma Aldrich*®) supplemented with 1 mM PMSF (#10837091001, *Roche*), 1 % Protease Inhibitor Cocktail (#P5726, *Sigma Aldrich*®), 1 % Phosphatase Inhibitor Cocktail 2 (#P5726, *Sigma Aldrich*®) and 1 % Phosphatase Inhibitor Cocktail 3 (#P0044, *Sigma Aldrich*®) just before use). Cell lysate was then transferred to a microcentrifuge tube and lysis completed by end-over-end rotation at 4 °C for 30 min. Afterwards, the cell lysate was cleared by centrifugation at 17,900×g for 20 min at 4 °C, and the supernatant transferred to a clean microcentrifuge tube. 10 % of this supernatant (~40 µL) was saved as part of the "whole-cell extract" fraction.

Once antibodies have successfully been conjugated to the Dynabeads™, the beads were pelleted by centrifugation at 700×g for 1 min at 4 °C. The supernatant was removed and beads washed with 200 µL of PBS-T, followed by centrifugation. The supernatant was removed and replaced with the cleared cell lysate, and the lysate-bead mixture was then incubated with end-over-end rotation at 4 °C for 2 h. The beads were pelleted and 10 % of the supernatant (~40 µL) was saved as part of the "flow-through" fraction. Unbound or non-precipitated proteins were washed away thrice (20 mM Tris-HCl pH = 8.0, 150 mM KCl, 10 % Triton X-100) from the beads, with centrifugation steps in between. Immunocomplexes were left bound to beads, which were resuspended in 50 µL of lysis buffer after the final wash. 10 % of the beads (~5 µL) were saved as part of the "bound" fraction. Proteins in the whole-cell extract, flow-through and bound fractions were denatured by heating in 1×Nu Page LDS Sample Buffer (#NP0007, Invitrogen™) supplemented with 10 % β-mercaptoethanol (#444203, Sigma Aldrich®) for 10 min at 70 °C. Western blotting was then performed to confirm immunoprecipitation efficiency (Fig. S5) prior to shipping the remaining of the bound fraction (~45 µL) to the *University of Bristol Proteomics Facility* (*University of Bristol*, UK).

Western blotting was performed with 10 % acrylamide/bis-acrylamide gels (#1610158, *Bio-Rad*). Proteins were immobilized onto polyvinylidene fluoride (PVDF) membranes (#IPVH00010, *Millipore*®) by a wet transfer method. Non-specific protein binding sites on PVDF membranes were blocked with a 5 % skimmed milk (#10651135, *Fisher Scientific*™) in 1×TBS (#T5030-50TAB, *Sigma Aldrich*®) with 0.01 % Tween®-20 (henceforth referred to as TBS-T) solution for 1 h at room temperature. Target proteins were immunolabelled with primary antibodies diluted 1:1,000 with 5 % skimmed milk in TBS-T. DyLight™ 680-conjugated secondary antibody (#35568, *Invitrogen*™) diluted 1:5,000 in 5 % skimmed milk in TBS-T was used to visualize the labelled proteins. Images captured using the C-Digit Li-Cor system (*LI-COR Bioscience*).

At the *University of Bristol Proteomics Facility*, the LC-MS samples were run on a 10 % SDS-PAGE gel until the dye front had migrated approximately 1 cm into the separating gel. Each gel lane was then subjected to in-gel tryptic digestion using a *DigestPro* automated digestion unit (*Intavis Ltd.*). The resulting peptides were fractionated using an

UltiMate™ 3000 nano-LC system in line with an LTQ-Orbitrap Velos mass spectrometer (*Thermo Scientific*™). Tandem mass spectra were acquired using the LTQ-Orbitrap Velos mass spectrometer controlled by *Xcalibur 2.1* software (*Thermo Scientific*™) and operated in data-dependent acquisition mode. The Orbitrap was set to analyze the survey scans at 60,000 resolution (at *m/z* 400) in the mass range 300 to 2000 *m/z* and the top 20 multiply charged ions in each duty cycle selected for MS/MS in the LTQ linear ion trap. The raw data files were processed and quantified using *Proteome Discoverer software* v1.4 (*Thermo Scientific*™) and searched against the *UniProt* Human database (downloaded September 2017: 139999 sequences) using the SEQUEST algorithm. The reverse database search option was enabled and all peptide data was filtered to satisfy false discovery rate (FDR) of 5 %.

Following the appropriate filtering steps outlined in Fig. S1 to identify true positive interacting proteins, *Pubmed* searches were manually performed in 2019, using as input the protein or gene name AND the term "Retina". The *Human Protein Atlas* [16–18] was used to confirm the organelle expression of proteins alongside *UniProtKB* [15]. *STRING* [14] and GO Cellular component analysis were performed by inputting LC-MS true positives hits into *STRING*, proteins were then automatically assigned GO terms. Protein fragments ID that were not recognized were manually searched and matched with the help of *UniProtKB* IDs.

2.4. Immunocytochemical staining

100,000 HEK293 cells were seeded onto 13-mm glass coverslips (#631-1578, *VWR*®) (within 6-well plates, 3 coverslips per well), transfected, fixed with 4 % PFA and washed with 1×PBS. Following fixation, coverslips were incubated with lysine blocking buffer (5 % horse serum (#26050088, *Gibco*™), 5 % goat serum (#16210072, *Gibco*™), 50 mM L-Lysine (#L5501, *Sigma Aldrich*®), 0.2 % Triton X-100 in 1×PBS) for 1 h at room temperature, and then primary antibody (diluted in Lysine buffer, see Table 1 for dilution) for 1 h at room temperature. Following three 1×PBS washes, 5 min each, coverslips were incubated with 1:400 diluted secondary antibody (diluted in lysine buffer) for 1 h at room temperature. Secondary antibodies were tested for potential non-specific staining (Fig. S6). Where necessary, 1:5,000 DAPI solution in 1×PBS (#D1306, *Invitrogen*^{TM}) was used to counterstain nuclei for 5 min prior to mounting. Coverslips were mounted with FluorSave mounting media (#345789, *Millipore*®). Cells were imaged with a *Leica TCS SP8* inverted confocal scanning microscope with a piezoelectric stage (*Leica Microsystems*) using a HC Plan Apochromat ×63 (1.4 NA) oil objective. Antibodies used in this study can be found in Table 1.

3. Method validation

3.1. Results

3.1.1. Identification of putative CLCC1-interacting proteins

CLCC1 has previously been shown to interact with Calreticulin and PIGBOS [7,13]. To further our understanding of the cellular functions of CLCC1 and infer how the Asp25Glu variant, which we have previously reported as being associated with RP [7], could impact CLCC1 function, we employed liquid chromatography with tandem mass spectrometry (LC-MS) to identify putative CLCC1 binding partners.

HEK293 cells were transfected with plasmids encoding FLAG-tagged CLCC1^{WT} or CLCC1^{Asp25Glu}, allowed to overexpress the fusion proteins, and then FLAG-tagged CLCC1$^{WT/\ Asp25Glu}$ were immunoprecipitated using anti-FLAG antibodies (Fig. 1A). Following elution of immunocomplexes, protein complexes containing CLCC1 were identified by LC-MS (Fig. 1B). An overview of how the LC-MS data was handled and filtering strategies used to construct CLCC1 interactomes is provided in Fig. S1. In brief, around 800 potential interactions were obtained for both the CLCC1^{WT} and Asp25Glu proteins. Filtering of out around 500 false positive interactions allowed us to identify 236 likely true positives with a cut off score $>$ 10 for CLCC1^{WT}, while for CLCC1^{Asp25Glu} we identified 249 immune complexes, that were considered true positives. 95 out of 236 immune complexes interacting with CLCC1^{WT} were not present as potential interactors of CLCC1^{Asp25Glu}, these were considered as interactions potentially lost in the Asp25Glu mutation.

To determine how the Asp25Glu variant impacts CLCC1 protein interactions and which cellular components it may localize to, we examined the gene ontology (GO) Cellular Component 2021 terms for putative CLCC1 interactors from the CLCC1^{WT} and CLCC1^{Asp25Glu} LC-MS datasets (Fig. 2). GO terms indicate that the majority of proteins co-precipitated with FLAG-tagged CLCC1^{WT} comprise ER proteins (59 %) or nuclear outer membrane-ER proteins (20 %) (Fig. 2). The interactome of the CLCC1^{Asp25Glu} mutant noticeably differs from CLCC1^{WT} protein. Several ER-related (37 %), cytoplasmic (28 %), endomembrane system (18 %) and organelle membrane (17 %) proteins were lost; and new interactions with cytoplasmic (40 %), ER-related (28 %), nuclear outer membrane-ER (14 %) and organelle membrane (18 %) proteins were detected with the CLCC1^{Asp25Glu} mutant relative to the CLCC1^{WT} protein (Fig. 2).

As CLCC1 appears to be important for retinal development and function, and the Asp25Glu variant is associated with RP [7], we analyzed the CLCC1 interactome further by attempting to identify CLCC1-interacting proteins that are enriched for retinal expression and may be relevant to retinal physiology. A cut-off score value of 10 (from the LC-MS data) was set for the list of putative CLCC1-interacting proteins, and the *PubMed* database was used to define which of these proteins have been previously reported as expressed in the retina. 39 potential CLCC1-interacting proteins were identified as expressed in the

Table 1
Antibodies used in this study.

Antibody Target	Catalog Number	Supplier	Host Species	Purpose	Dilution
FLAG	F1804	*Sigma-Aldrich*	Mouse	LC-MS Immunocytochemistry	1:1,000 1:100
FLAG (DyLight™ 680-Conjugated)	MA1-91878-D680	*Invitrogen*	Mouse	Western Blotting	1:1,000
CLCC1	HPA013210	*Atlas*	Rabbit	Immunocytochemistry	1:100
Calnexin	ab31290	*Abcam*	Mouse	Immunocytochemistry	1:100
SigmaR1	ab53852	*Abcam*	Rabbit	Immunocytochemistry	1:50
Calreticulin	PA3-900	*Invitrogen*	Rabbit	Immunocytochemistry	1:100
GAPDH	sc-47724	*Santa Cruz Biotechnology*	Mouse	Western Blotting	1:1,000
Anti-Mouse (Alexa Fluor® 488-Conjugated)	A-32723	*Invitrogen*	Goat	Immunocytochemistry	1:400
Anti-Rabbit (Alexa Fluor® 647-Conjugated)	A-32795	*Invitrogen*	Donkey	Immunocytochemistry	1:400
Anti-Mouse (DyLight™ 680-Conjugated)	35568	*Invitrogen*	Goat	Western Blotting	1:5,000

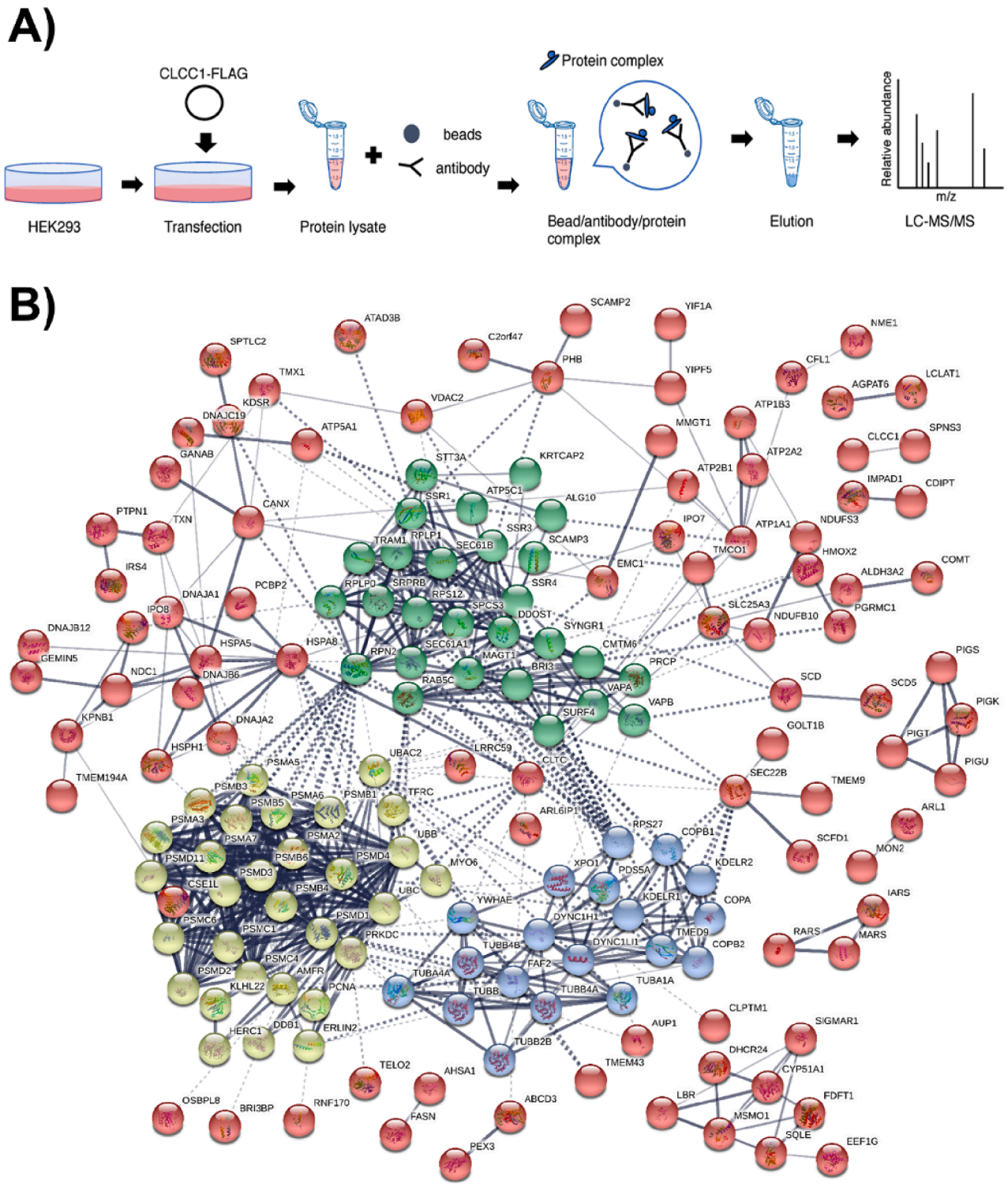

Fig. 1. Immunoprecipitation and LC-MS to identify putative CLCC1-interacting proteins. A) Overview of immunoprecipitation workflow, where adherent HEK293 cells are transfected with plasmid vectors encoding FLAG-tagged CLCC1^{WT} or CLCC1^{Asp25Glu}, and the expressed proteins are pulled down with anti-FLAG antibody-conjugated beads. Any binding partners that co-precipitate with CLCC1$^{WT/Asp25Glu}$ are detected by LC-MS. Created with BioRender.com. B) Overview of 'true positive', more likely true CLCC1^{WT}-interacting proteins detected by LC-MS. The light green cluster contains protein related to the proteasome, the dark green cluster is composed of proteins related to the ER, while the blue cluster indicates proteins involved in intracellular transport. Proteins in red do not belong to a particular cluster. Created with *STRING* [14]. (For interpretation of the references to colour in this figure legend, the reader is referred to the web version of this article.)

retina (Fig. 3A). Of these, 4 were detected exclusively in the CLCC1^{WT} dataset (CLTC, FASN, ALDH3A2, and EMC1); 12 were detected exclusively in the CLCC1^{Asp25Glu} dataset (LDHA, LDHB, PRDX1, YWHAQ, RPN1, CS, DHCR7, NSDHL, PSMD13, YWHAZ, RPS5, and PYCR1); and 23 were commonly co-precipitated with the CLCC1^{WT} and CLCC1^{Asp25Glu} proteins (TUBB4B, HSPA5, HSPA8, UBC, TUBA1A, ATP2A2, SLC27A4, ATP1A1, XPO1, SGMR1, CALX, PHB, PGRMC1, PSMC1, PSMB5, VDAC2, SLC29A1, YWHAE, ATP2B1, PSMA5, IPO8 and CDIPT)

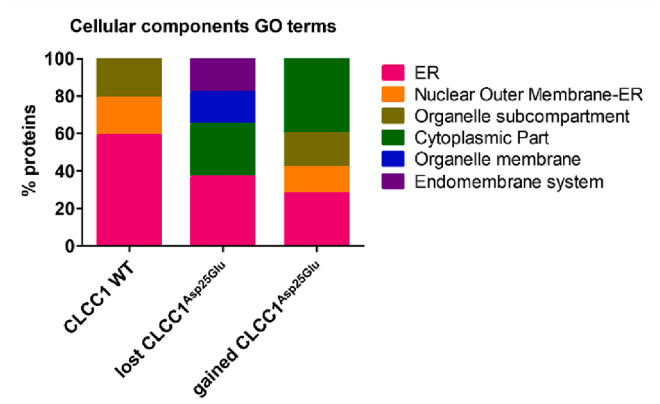

Fig. 2. The Asp25Glu variant in CLCC1 results in increased interactions with cytoplasmic proteins. Comparison of GO Cellular Component 2021 term enrichment in proteins that interact with CLCC1^{WT} but not the CLCC1^{Asp25Glu} mutant ("lost CLCC1 Asp25Glu") and proteins that interact with the CLCC1^{Asp25Glu} mutant but not the CLCC1^{WT} protein ("gained CLCC1 Asp25Glu") relative to the GO Cellular Component terms for CLCC1^{WT}-interacting proteins. GO Cellular Component 2021 enrichment analysis performed in *STRING* [14].

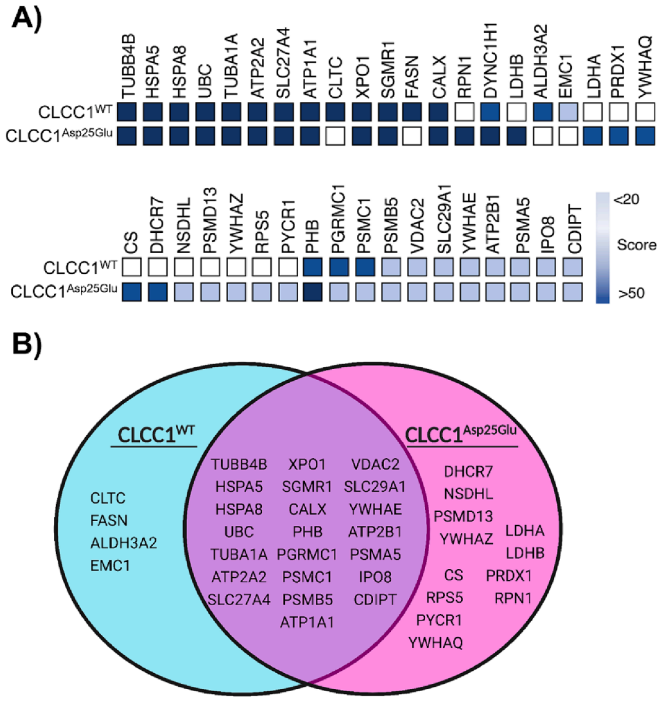

Fig. 3. Retinal expressed proteins interacting with CLCC1^{WT} and the CLCC1^{Asp25Glu} mutant. A) Coulson plot of CLCC1-interacting proteins reported as expressed in the retina from a *Pubmed* search. The scores of a protein from the LC-MS data are expressed in shades of blue; the darker the blue = the higher the score; the lighter the blue = the lower the score; unshaded box = not detected as interacting with CLCC1^{WT} or CLCC1^{Asp25Glu} respectively. B) Venn diagram visualizing the unique and shared binding partners of the wild-type and Asp25Glu mutant CLCC1 proteins; summarizes the results from part A). Created with BioRender.com. (For interpretation of the references to colour in this figure legend, the reader is referred to the web version of this article.)

(Fig. 3B).

We then subdivided the 39 retina-expressed CLCC1-interacting proteins based on subcellular localization according to the *UniProtKB* [15] and *Human Protein Atlas* [16–18] databases. The compartment most represented in this list was the cytosol, followed by the ER, nucleus, plasma membrane and mitochondria (Fig. 4). Only a few CLCC1-interacting proteins were associated with endosome (UBC, PHB, CLTC and ATP2B1), Golgi apparatus (FASN, CDIPT and ATP2B1), vesicles (XPO1 and PHB), and peroxisome and lysosome (ALDH3A2, CS and CLTC) compartment localization.

3.1.2. *CLCC1 interacts with SigmaR1 at MAMs*

Following analysis of the LC-MS data, two proteins of interest were chosen for follow-up investigation: Calnexin and SigmaR1. Calnexin is a transmembrane calcium-binding protein [19] binding partially folded glycoproteins to determine if they can be released from the ER or sent to the proteasome [20]. Calnexin also controls intracellular Ca^{2+} oscillation via interaction with SERCA pumps [21]. SigmaR1 is a receptor localized in MAMs [22], where calcium handling proteins such as IP_3 receptors are highly compartmentalized [23]. SigmaR1 has previously been associated with hereditary motor neuropathy and amyotrophic lateral sclerosis [24,25] and is known to be expressed in the retina [26]. Hence, both Calnexin and SigmaR1 are important proteins for the UPR and Ca^{2+} homeostasis.

To validate the LC-MS findings, we examined the localization of CLCC1 with selected proteins in HEK293 and NIH/3T3 cells. Endogenous staining for CLCC1 in NIH/3T3 cells shows a degree of co-localization with Calnexin, supporting the existence of CLCC1/Calnexin protein complexes (Figs. 5A and S2A). This likely occurs at the ER, and further cements CLCC1 as an ER-associated protein.

To test if CLCC1 interacts with SigmaR1 at the ER, and if the Asp25Glu variant affects this localization, NIH/3T3 cells were transfected with constructs encoding the FLAG-tagged CLCC1^{WT} and CLCC1^{Asp25Glu} proteins as well as mCherry containing a KDEL motif (referred to as mCherry-KDEL; KDEL is an ER retention signal which targets mCherry to the ER [27]. Immunostaining for SigmaR1 in the transfected cells revealed a punctate pattern similar to both CLCC1^{WT} and CLCC1^{Asp25Glu} proteins (Fig. 5B and S2B). CLCC1^{WT} and CLCC1^{Asp25Glu} appear to associate in close proximity with SigmaR1 puncta, and these complexes partially co-localize with mCherry-KDEL – indicating likely CLCC1/SigmaR1 interactions at the ER (Fig. 5B). The lack of complete co-localization with mCherry-KDEL suggests potential interactions of CLCC1 with SigmaR1 not located directly at the ER but at contact sites (e.g., between the ER and mitochondria). This was tested by treatment with MitoTracker™ Red, which showed that CLCC1 and SigmaR1 may associate at regions between the ER and mitochondria (Fig. 5C and S2C), consistent with CLCC1 being located at ER-mitochondria membrane contact sites (or MAM). This agrees with reported CLCC1/PIGBOS interactions at MAMs [13]. As a positive control for immunostaining, we show that CLCC1 co-localizes with Calreticulin (Fig. 5D and S2D), as expected from our previous work [7]. These findings confirm that CLCC1 is an ER and MAM-associated protein, and that the Asp25Glu variant does not appear to prevent interactions with SigmaR1 or associations with the ER and MAMs.

We also note that *CLCC1* is predicted to produce four different isoforms by alternative splicing (Fig. S3A and B) [15] and that these other CLCC1 isoforms co-localize with Calreticulin when expressed in HEK293 cells (Fig. S4). This indicates that not only the canonical isoform but other products of the *CLCC1* gene are ER-associated proteins. Whether other isoforms of CLCC1 can interact with SigmaR1 or are localized to MAMs will require further investigation.

4. Discussion

Through the findings of this study, we have gained new insights into the cellular localization and functional role of CLCC1. Using LC-MS, we uncovered that CLCC1 predominantly engages with proteins localized to the nuclear outer membrane-ER boundary. This finding aligns with our immunostaining data indicating a concentration of CLCC1 in the perinuclear space. To examine whether and how the Asp25Glu variant associated with RP [7] impacts CLCC1 function, we carried out a

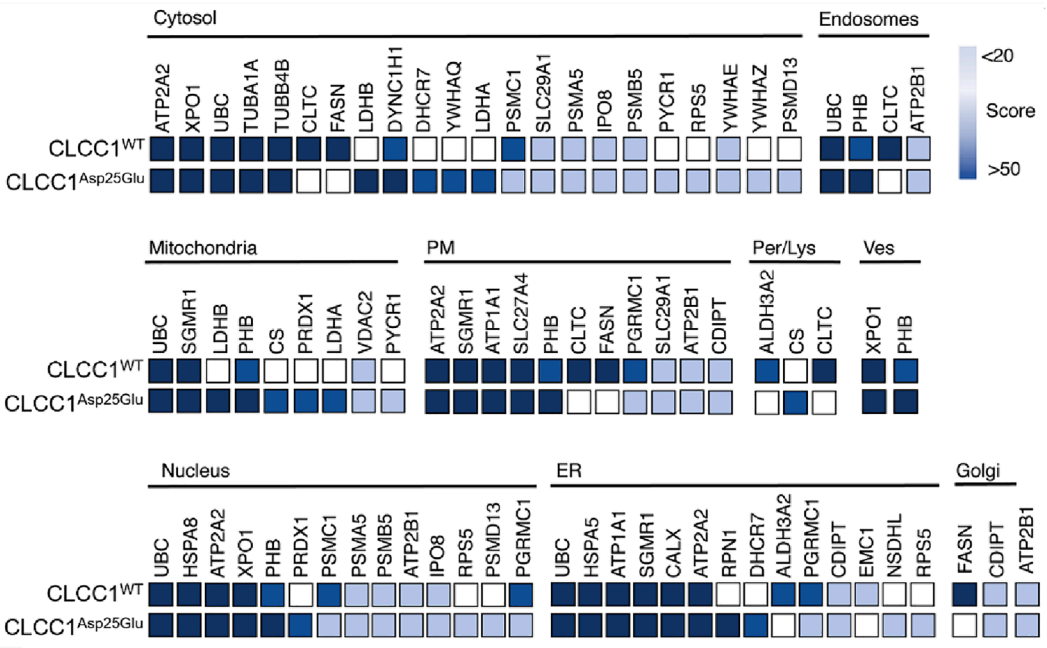

Fig. 4. Subdivision of CLCC1 binding partners based on their intracellular compartmentalization. Coulson plots displaying the range of subcellular localizations of CLCC1^{WT} and CLCC1^{Asp25Glu} –interacting proteins. Protein localization was determined using data available from the *UniProtKB* [15] and *Human Protein Atlas* [16–18] databases. The scores of a protein from the LC-MS data are expressed in shades of blue; the darker the blue = the higher the score; the lighter the blue = the lower the score; unshaded box = not detected as interacting with CLCC1^{WT} or CLCC1^{Asp25Glu} respectively. (For interpretation of the references to colour in this figure legend, the reader is referred to the web version of this article.)

comparative analysis of the distribution of GO Cellular Component terms among CLCC1-interacting proteins. This analysis provides evidence that the CLCC1^{Asp25Glu} mutant has altered protein interactions, signified by an increase in cytoplasmic protein interactions. Our results demonstrate that the wild-type and mutant CLCC1 proteins bind differentially to a subset of known retinal expressed proteins in different cellular compartments, further supporting a shift in cellular localization of the Asp25Glu mutant. Interestingly, the region of the N-terminus tail of CLCC1 affected by the Asp25Glu variant is cytoplasmic (Fig. S3A and B), suggesting the difference in CLCC1^{WT} and CLCC1^{Asp25Glu} interactomes could be attributed to some change in the structure of the cytoplasmic N-terminus tail.

In order to substantiate the findings obtained through LC-MS, we scrutinized two prospective CLCC1 interactors, namely Calnexin and SigmaR1, employing immunocytochemical staining and fluorescence microscopy techniques. Both Calnexin and SigmaR1 can be found associated with the ER and with MAMs [28]. Consistent with the LC-MS data, both Calnexin and SigmaR1 co-localize with CLCC1. By co-labelling of the ER and mitochondria, we show that CLCC1 associates with SigmaR1 at the ER and at MAMs, reinforcing CLCC1 as a component of MAMs.

The precise manner in which the gain or loss of protein interactors by the CLCC1^{Asp25Glu} mutant influences the pathogenesis of RP remains enigmatic, albeit several intriguing targets have already surfaced in our dataset. For example, the CLCC1^{Asp25Glu} mutant appears to have gained the capability to interact with LDHA and LDHB, lactate dehydrogenase enzymes expressed in the retina that play essential roles in the maintenance of retinal health [29]. Furthermore, the CLCC1^{Asp25Glu} mutant also seems to lose interactions with ALDH3A2 and EMC1, proteins associated with retinal degeneration [30–34]. It would be pertinent for future research to validate the loss or gain of CLCC1 interactors in retinal cell types and investigate how these could impact protein localization, cell functionality or response to particular stressors relevant to RP.

Nonetheless, it is of importance to acknowledge the potential limitations of the LC-MS data. For instance, Calreticulin, which we have previously shown to interact with CLCC1 [7] and replicated in this study, is not present in both the lists of CLCC1^{WT}- or CLCC1^{Asp25Glu} -interacting proteins. This could indicate that the LC-MS technique may not entirely be reliable or that the current sample processing workflow (e.g., choice of lysis buffer composition) was not suitable for capturing CLCC1/Calreticulin interactions. Hence, it is imperative to validate targets identified via LC-MS wherever feasible.

Despite its limitations, the LC-MS data produced in this study will undoubtedly serve as a valuable resource for future inquiries into the cellular function of CLCC1, both within the sphere of retinal development, health or function and beyond. The investigation of the CLCC1^{Asp25Glu} variant in our study lays the groundwork for further decoding of the influence that the Asp25Glu variant may exert on CLCC1 interactivity and consequently, retinal cell function in the context of RP.

Limitations

Not Applicable.

Ethics statements

Our research, "Unraveling CLCC1 Interactome: Impact of Asp25Glu Variant and Its Interaction with SigmaR1 at the Mitochondrial-Associated ER Membrane (MAM)," did not involve human subjects, animal experiments, or the use of social media data. Accordingly, the specific ethical guidelines related to these areas as outlined by MethodsX do not apply. We ensure that our study was conducted with a commitment to ethical scientific practices.

CRediT authorship contribution statement

Ilaria D'Atri: Writing – original draft, Visualization, Project administration, Methodology, Investigation, Formal analysis, Data curation, Conceptualization. **Emily-Rose Martin:** Formal analysis, Validation, Visualization, Writing – original draft, Writing – review & editing. **Liming Yang:** Writing – review & editing, Visualization, Validation, Investigation. **Elizabeth Sears:** Visualization, Validation,

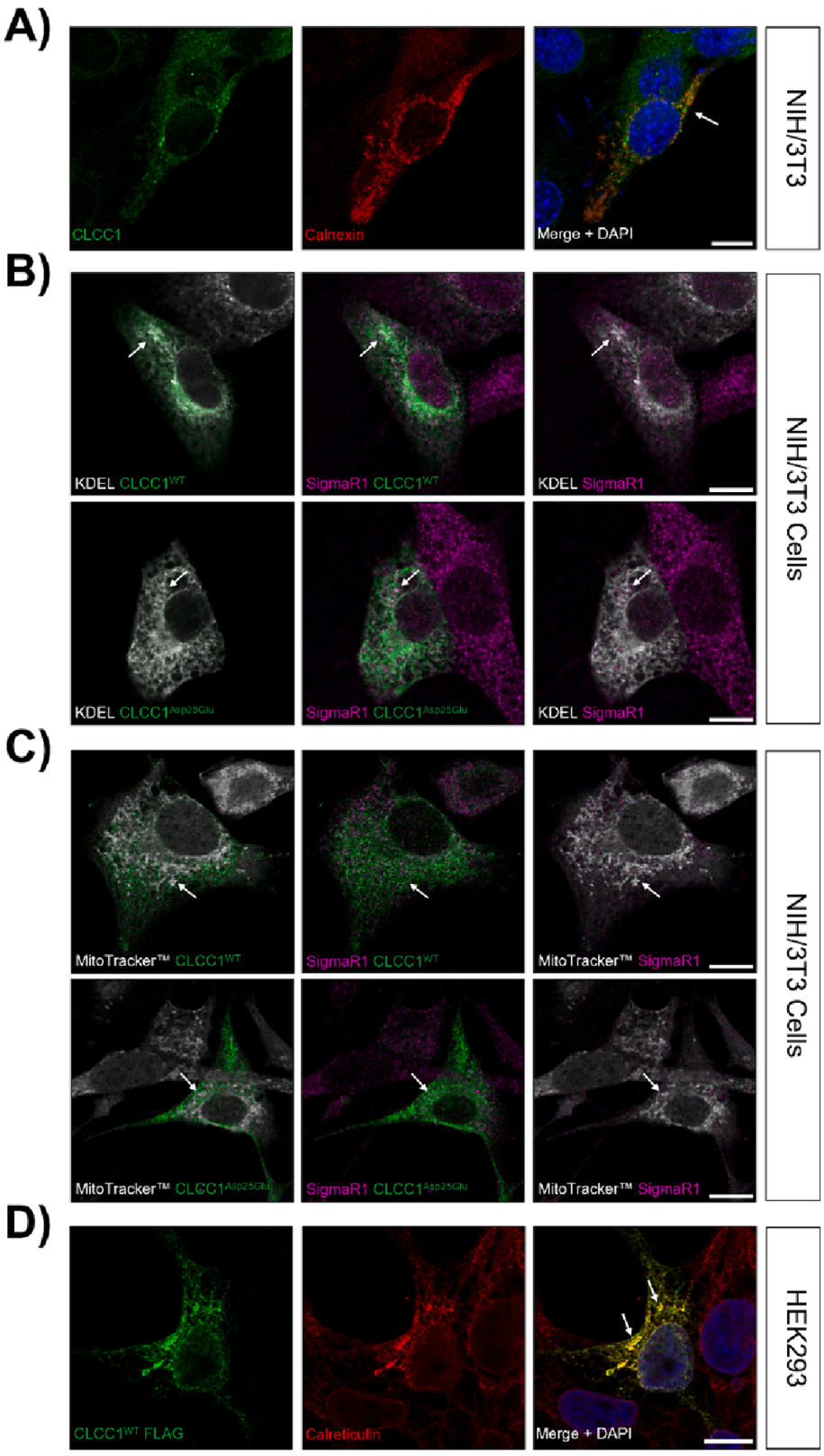

Fig. 5. CLCC1 forms complexes with Calnexin and SigmaR1 and localizes to the ER and MAMs. A) Co-staining of endogenous CLCC1 and Calnexin in NIH/3T3 cells. Nuclei counterstained with DAPI. Arrow = example of CLCC1 and Calnexin co-localization. B) Staining for endogenous SigmaR1 in NIH/3T3 cells co-expressing mCherry-KDEL and yellow fluorescent protein (YFP)-tagged CLCC1^{WT} or CLCC1^{Asp25Glu} proteins. Arrows = examples of CLCC1 and SigmaR1 association at the ER. C) Staining for SigmaR1 in NIH/3T3 cells expressing YFP-tagged CLCC1^{WT} or CLCC1^{Asp25Glu} proteins following treatment with MitoTracker™ Red. Arrows = examples of CLCC1 and SigmaR1 association at MAMs. D) Co-staining for FLAG and endogenous Calreticulin in HEK293 cells expressing FLAG-tagged CLCC1^{WT}. Nuclei counterstained with DAPI. Arrows = examples of CLCC1 and Calreticulin co-localization. Scale bars = 10 μm. (For interpretation of the references to colour in this figure legend, the reader is referred to the web version of this article.)

Investigation. **Emma Baple:** Supervision, Investigation, Conceptualization. **Andrew H. Crosby:** Data curation, Conceptualization, Funding acquisition, Project administration, Resources, Software, Supervision. **John K. Chilton:** Supervision, Software, Resources, Project administration, Investigation, Conceptualization, Data curation. **Asami Oguro-Ando:** Project administration, Methodology, Investigation, Funding acquisition, Formal analysis, Data curation, Conceptualization, Supervision, Validation, Visualization, Writing – review & editing, Resources, Software.

Declaration of competing interest

The authors declare that they have no known competing financial interests or personal relationships that could have appeared to influence the work reported in this paper.

Data availability

No data was used for the research described in the article.

Acknowledgements

This work was supported (in part) by charities Gift of Sight/Fight For Sight (Reference 2027). The authors would like to thank Connor Horton and Kate Heesom for their assistance with the LC-MS experiments. The authors are also grateful to Kate Ellacott for kindly gifting us the Mito-Tracker™ used in this study. Finally, the authors would like to acknowledge the insightful discussions and support given by Josan Gandawijaya.

Appendix A. Supplementary data

Supplementary data to this article can be found online at https://doi.org/10.1016/j.neulet.2024.137778.

References

[1] I. Braakman, D.N. Hebert, Protein folding in the endoplasmic reticulum, Cold Spring Harb. Perspect. Biol. 5 (5) (2013) a013201.
[2] A.D. Gillon, C.F. Latham, E.A. Miller, Vesicle-mediated ER export of proteins and lipids, Biochim. Biophys. Acta (BBA) – Mol. Cell Biol. Lipids 1821 (8) (2012) 1040–1049.
[3] D.S. Schwarz, M.D. Blower, The endoplasmic reticulum: structure, function and response to cellular signaling, Cell. Mol. Life Sci. 73 (1) (2016) 79–94.
[4] I. Kim, W. Xu, J.C. Reed, Cell death and endoplasmic reticulum stress: disease relevance and therapeutic opportunities, Nat. Rev. Drug Discov. 7 (12) (2008) 1013–1030.
[5] C.M. Oslowski, F. Urano, Measuring ER stress and the unfolded protein response using mammalian tissue culture system, Methods Enzymol. [Internet]. 490 (C) (2011) 71. Available from: /pmc/articles/PMC3701721/.
[6] C.M. Oslowski, F. Urano, The binary switch between life and death of ER stressed beta cells, Curr. Opin. Endocrinol. Diabetes Obes. [Internet] 17 (2) (2010) 107. Available from: /pmc/articles/PMC2898716/.
[7] L. Li, X. Jiao, I. D'Atri, F. Ono, R. Nelson, C.C. Chan, et al., Mutation in the intracellular chloride channel CLCC1 associated with autosomal recessive retinitis pigmentosa, PLoS Genet. [Internet]. 14 (8) (2018). Available from: https://journals.plos.org/plosgenetics/article?id=10.1371/journal.pgen.1007504.
[8] D. Athanasiou, M. Aguila, J. Bellingham, W. Li, C. McCulley, P.J. Reeves, et al., The molecular and cellular basis of rhodopsin retinitis pigmentosa reveals potential strategies for therapy, Prog. Retin. Eye Res. [Internet]. 62 (1) (2018). Available from: /pmc/articles/PMC5779616/.
[9] T. Yamashita, J. Liu, J. Gao, S. LeNoue, C. Wang, J. Kaminoh, et al., Essential and synergistic roles of RP1 and RP1L1 in rod photoreceptor axoneme and retinitis pigmentosa, J. Neurosci. [Internet]. 29 (31) (2009) 9748. Available from: /pmc/articles/PMC2748320/.
[10] H. Kroeger, J.M.D. Grandjean, W.C.J. Chiang, D.D. Bindels, R. Mastey, J. Okalova, et al., ATF6 is essential for human cone photoreceptor development, Proc. Natl. Acad. Sci. U. S. A. [Internet] 118 (39) (2021) e2103196118. Available from: https://www.pnas.org/doi/abs/10.1073/pnas.2103196118.
[11] L. Guo, Q. Mao, J. He, X. Liu, X. Piao, L. Luo, et al., Disruption of ER ion homeostasis maintained by an ER anion channel CLCC1 contributes to ALS-like pathologies, Cell Res [Internet]. 33 (7) (2023). Available from: https://pubmed.ncbi.nlm.nih.gov/37142673/.
[12] Y. Jia, T.J. Jucius, S.A. Cook, S.L. Ackerman, Loss of Clcc1 results in ER stress, misfolded protein accumulation, and neurodegeneration, J. Neurosci. [Internet] 35 (7) (2015) 3001–3009. Available from https://pubmed.ncbi.nlm.nih.gov/25698737/.
[13] Q. Chu, T.F. Martinez, S.W. Novak, C.J. Donaldson, D. Tan, J.M. Vaughan, et al., Regulation of the ER stress response by a mitochondrial microprotein, Nat. Commun. [Internet] 10 (1) (2019). Available from: https://pubmed.ncbi.nlm.nih.gov/31653868/.
[14] D. Szklarczyk, A.L. Gable, D. Lyon, A. Junge, S. Wyder, J. Huerta-Cepas, et al., STRING v11: protein-protein association networks with increased coverage, supporting functional discovery in genome-wide experimental datasets, Nucleic Acids Res. [Internet] 47 (D1) (2019) D607–D613. Available from: https://pubmed.ncbi.nlm.nih.gov/30476243/.
[15] The UniProt Consortium, A. Bateman, M.J. Martin, S. Orchard, M. Magrane, S. Ahmad, et al., UniProt: the Universal Protein Knowledgebase in 2023, Nucleic Acids Res. [Internet] (2023) D523–D531. Available from: https://academic.oup.com/nar/article/51/D1/D523/6835362.
[16] M. Uhlen, P. Oksvold, L. Fagerberg, E. Lundberg, K. Jonasson, M. Forsberg, et al., Towards a knowledge-based Human Protein Atlas, Nat. Biotechnol. 28 (12) (2010) 1248–1250. Available from https://www.nature.com/articles/nbt1210-1248.
[17] M. Uhlén, L. Fagerberg, B.M. Hallström, C. Lindskog, P. Oksvold, A. Mardinoglu, et al., Tissue-based map of the human proteome, Science (1979) [Internet] 347 (6220) (2015). Available from: https://www.science.org/doi/10.1126/science.1260419.
[18] M. Uhlén, E. Björling, C. Agaton, C.A.K. Szigyarto, B. Amini, E. Andersen, et al., A human protein atlas for normal and cancer tissues based on antibody proteomics, Mol. Cell. Proteom. [Internet] 4 (12) (2005) 1920–1932. Available from: http://www.mcponline.org/article/S1535947620300281/fulltext.
[19] G. Kozlov, K. Gehring, Calnexin cycle – structural features of the ER chaperone system, FEBS J. [Internet] 287 (20) (2020) 4322. Available from: /pmc/articles/PMC7687155/.
[20] L. Lamriben, J.B. Graham, B.M. Adams, D.N. Hebert, N-glycan-based ER molecular chaperone and protein quality control system: The calnexin binding cycle, Traffic [Internet]. 17 (4) (2016) 308–326. Available from https://pubmed.ncbi.nlm.nih.gov/26676362/.
[21] H.L. Roderick, J.D. Lechleiter, P. Camacho, Cytosolic phosphorylation of calnexin controls intracellular Ca(2+) oscillations via an interaction with SERCA2b, J. Cell Biol. [Internet]. 149 (6) (2000) 1235–1247. Available from https://pubmed.ncbi.nlm.nih.gov/10851021/.
[22] B. Delprat, L. Crouzier, T.P. Su, T. Maurice, At the crossing of ER stress and MAMs: A key role of sigma-1 receptor? Adv. Exp. Med. Biol. [Internet]. 1131 (2020) 699–718. Available from: https://pubmed.ncbi.nlm.nih.gov/31646531/.
[23] E. Kania, G. Roest, T. Vervliet, J.B. Parys, G. Bultynck, IP3 receptor-mediated calcium signaling and its role in autophagy in cancer, Front. Oncol. 7 (Jul) (2017).
[24] A. Al-Saif, F. Al-Mohanna, S. Bohlega, A mutation in sigma-1 receptor causes juvenile amyotrophic lateral sclerosis, Ann. Neurol. [Internet]. 70 (6) (2011) 913–919. Available from: https://pubmed.ncbi.nlm.nih.gov/21842496/.
[25] E. Gregianin, G. Pallafacchina, S. Zanin, V. Crippa, P. Rusmini, A. Poletti, et al., Loss-of-function mutations in the SIGMAR1 gene cause distal hereditary motor neuropathy by impairing ER-mitochondria tethering and Ca2+ signalling, Hum. Mol. Genet [Internet]. 25 (17) (2016) 3741–3753. Available from: https://pubmed.ncbi.nlm.nih.gov/27402882/.
[26] T.A. Mavlyutov, M. Epstein, L.W. Guo, Subcellular localization of the sigma-1 receptor in retinal neurons — an electron microscopy study, Sci. Rep. [Internet]. (2015) 5. Available from: /pmc/articles/PMC4649997/.
[27] N. Zurek, L. Sparks, G. Voeltz, Reticulon short hairpin transmembrane domains are used to shape ER tubules, Traffic [Internet]. 12 (1) (2011) 28. Available from: /pmc/articles/PMC3005309/.
[28] T. Simmen, M.S. Herrera-Cruz, Plastic mitochondria-endoplasmic reticulum (ER) contacts use chaperones and tethers to mould their structure and signaling, Curr. Opin. Cell Biol. 1 (53) (2018) 61–69.
[29] A. Rajala, M.A. Bhat, K. Teel, G.K. Gopinadhan Nair, L. Purcell, R.V.S. Rajala, The function of lactate dehydrogenase A in retinal neurons: implications to retinal degenerative diseases, PNAS Nexus [Internet]. 2 (3) (2023). Available from: https://pubmed.ncbi.nlm.nih.gov/36896135/.
[30] L.H. Lambert, N. Shaikh, J.L. Marx, D.J. Ramsey, End-stage crystalline maculopathy with retinal atrophy in Sjögren-Larsson syndrome: a case report and review of the literature, Therap. Adv. Rare Dis. [Internet]. 3 (2022). Available from: https://pubmed.ncbi.nlm.nih.gov/37180414/.
[31] P.S. Bindu, Sjogren-Larsson syndrome: mechanisms and management, Appl. Clin. Genet. [Internet]. 13 (2020) 13–24. Available from: https://pubmed.ncbi.nlm.nih.gov/32021380/.
[32] S. Fouzdar-Jain, D.W. Suh, W.B. Rizzo, Sjögren-Larsson syndrome: a complex metabolic disease with a distinctive ocular phenotype, Ophthal. Genet. [Internet]. 40 (4) (2019) 298–308. Available from: https://pubmed.ncbi.nlm.nih.gov/31512987/.
[33] S.N. Al-Holou, E. Siefker, S. Fouzdar-Jain, D.W. Suh, W.B. Rizzo, Macular crystalline inclusions in Sjögren-Larsson syndrome are dynamic structures that undergo remodeling, Ophthal. Genet. [Internet]. 41 (4) (2020) 381–385. Available from: https://pubmed.ncbi.nlm.nih.gov/32506993/.
[34] X. Li, Z. Jiang, Y. Su, K. Wang, X. Jiang, K. Sun, et al., Deletion of Emc1 in photoreceptor cells causes retinal degeneration in mice, FEBS J. [internet]. (2023). Available from: https://onlinelibrary.wiley.com/doi/full/10.1111/febs.16807.